The Amide Oxygen as a Donor Group. Metal Ion Complexing Properties of Tetra-*N*-acetamide Substituted Cyclen: A Crystallographic, NMR, Molecular Mechanics, and Thermodynamic Study

Hulisani Maumela,[†] Robert D. Hancock,*[,†] Laurence Carlton,[†] Joseph H. Reibenspies,[‡] and Kevin P. Wainwright[§]

Contribution from the Departments of Chemistry, University of the Witwatersrand, WITS 2050, Johannesburg, South Africa, Texas A&M University, College Station, Texas 77843, and The Flinders University of South Australia, G.P.O. Box 2100, Adelaide, South Australia 5001

Received November 15, 1994[⊗]

Abstract: The syntheses of the octadentate ligand DOTAM (1,4,7,10-tetrakis(acetamido)-1,4,7,10-cyclododecane) and its complexes with Zn(II), Cd(II), and Ca(II) are described. Crystal structures of $[Cd(DOTAM)](ClO_4)_2 \cdot 1.5H_2O$ (**1**), $[Ca(DOTAM)](ClO_4)_2 \cdot 2.5H_2O$ (**2**), and $[Zn(DOTAM)](ClO_4)_2 \cdot H_2O$ (**3**) are reported. Crystal data: (**1**) monoclinic, space group *Cc*, $a = 11.908(2)$ Å, $b = 21.237(3)$ Å, $c = 11.445(2)$ Å, $\beta = 102.15(1)°$; (**2**) monoclinic, $P2_1/c$, $a = 14.031(9)$ Å, $b = 11.469(8)$ Å, $c = 17.448$ Å, $\beta = 92.10(1)°$; (**3**) triclinic, space group $P\bar{1}$, $a = 9.490(1)$ Å, $b = 12.464(2)$ Å, $c = 12.998(2)$ Å, $\alpha = 99.070(1)°$, $\beta = 107.67(1)°$, and $\gamma = 108.24(1)°$. There is an unusual distortion in the coordination geometry of the complexes. There are two sets of metal-to-oxygen bond lengths for each complex; Zn(II) has two oxygens, placed opposite each other in the approximately square arrangement defined by the four oxygen donor atoms at about 2.19 Å and two at 3.23 Å, Cd(II) has two at 2.34 and two at 2.64 Å, and Ca(II) has two at 2.40 Å and two at 2.42 Å. Molecular mechanics calculations suggest the Cd(II) and Zn(II) structures represent six coordination of four nitrogens and two of the oxygens, while the two long bonds represent van der Waals contacts with a possible electrostatic component. Approach of the oxygen donors to the metal ion is controlled by the van der Waals radii of the oxygens. ^{13}C NMR studies give rates of helicity interchange of the complexes Zn(II) > Hg(II) > Cd(II) > Ca(II) ≫ Pb(II). This order is discussed in terms of the difference in bond lengths between the two sets of oxygen donors. A stability constant study gave $\log K_1$ values in 0.1 M $NaNO_3$ and 25 °C: Cu(II), 16.3; Zn(II), 10.47; Ca(II), 7.54; Sr(II), 6.67; Ba(II), 5.35; Hg(II), 14.53; La(III), 10.35; Gd(III), 10.05. For Cd(II) and Pb(II), the complexes were fully formed even at pH 0.3, and only a lower limit of 19 for $\log K_1$ could be set. Selectivity of DOTAM for metal ions is discussed in terms of coordinating properties of the amide oxygen donor and geometric requirements of the DOTAM ligand.

For several years the present authors have been interested in the effect that the neutral oxygen donor has on the selectivity of metal ions for ligands.[1-11] It seems clear that addition of donor groups that contain neutral oxygen donors to ligands alters selectivity in favor of larger relative to smaller metal ions. This effect seems[8] to derive from the fact that neutral oxygen donors are almost invariably added to ligands in such a way that five-membered chelate rings are formed on complex formation. Extensive studies have shown[12,13] that five-membered chelate rings promote selectivity for larger metal ions, while six-membered chelate rings promote selectivity for smaller metal ions. Ligand design efforts focussed on development of ligands selective for the toxic heavy metal ions Cd(II) and Pb(II) have resulted in the ligand DOTHP seen in Figure 1. This ligand has shown considerable selectivity for the large Cd(II) ion over the small Zn(II) ion in thermodynamic studies.[4] It is the selectivity for large metal ions over Zn(II) in biomedical applications that appears to be the most important thing to achieve in many situations. For example, there is evidence that toxicity of Gd(III) complexes for MRI applications correlates[14] with the difference between $\log K_1$ for the Gd(III) and the Zn(II) complexes, rather than the absolute stability of the complex with Gd(III). The inference here is that toxicity of the Gd(III) complexes derives, at least in part, from displacement of the toxic Gd^{3+} ion from its complex by Zn(II). The DOTHP ligand has also shown considerable promise in animal studies[15] for

[†] University of the Witwatersrand.
[‡] Texas A&M University.
[§] The Flinders University.
[⊗] Abstract published in *Advance ACS Abstracts*, June 1, 1995.

(1) Thom, V. J.; Shaikjee, M. S.; Hancock, R. D. *Inorg. Chem.* **1986**, *25*, 2992-3000.
(2) Damu, K.; Shaikjee, M. S.; Michael, J. P.; Howard, A. S.; Hancock, R. D. *Inorg. Chem.* **1986**, *25*, 3879-3883.
(3) Hancock, R. D. *Pure Appl. Chem.* **1986**, *58*, 1445-1452.
(4) Hancock, R. D.; Shaikjee, M. S.; Dobson, S. M.; Boeyens, J. C. A. *Inorg. Chim. Acta* **1988**, *154*, 229-238.
(5) Hancock, R. D.; Bhavan, R.; Wade, P. W.; Boeyens, J. C. A.; Dobson, S. M. *Inorg. Chem.* **1989**, *28*, 187-194.
(6) Hancock, R. D.; Martell, A. E. *Chem. Rev.* **1989**, *89*, 1875-1914.
(7) Damu, K. V.; Hancock, R. D.; Wade, P. W.; Boeyens, J. C. A.; Billing, D. G.; Dobson, S. M. *J. Chem. Soc., Dalton Trans.* **1991**, *293*-298.
(8) Hancock, R. D. In *Perspectives in Inorganic Chemistry*; Williams, A. P., Floriani, C., Merbach, A. E., Eds.; VCH Publishers: Weinheim; Verlag. Helv. Chim. Acta, Basel, 1992; pp 129-151.
(9) Hancock, R. D. *Pure Appl. Chem.* **1993**, *65*, 941-946.
(10) Pittet, P.-A.; Laurence, G. S.; Lincoln, S. F.; Turonek, M. L.; Wainwright, K. P. *J. Chem. Soc., Chem. Commun.* **1991**, 1205-1206.
(11) Hancock, R. D. *J. Inclusion Phenom. Mol. Recognit. Chem.* **1994**, *17*, 63-80.
(12) Hancock, R. D. *J. Chem. Educ.* **1992**, *69*, 615-621.
(13) Hancock, R. D. *Prog. Inorg. Chem.* **1989**, *37*, 187-291.
(14) Cacheris, W. P.; Quay, S. C.; Racklage, S. M. *Magn. Reson. Imaging* **1990**, *8*, 467-481.
(15) Gulumian, M.; Casimiro, E.; Rama, D. B. K.; Linder, P., W.; Hancock, R. D. *Hum. Exp. Toxicol.* **1993**, *12*, 247-251.

0002-7863/95/1517-6698$09.00/0 © 1995 American Chemical Society

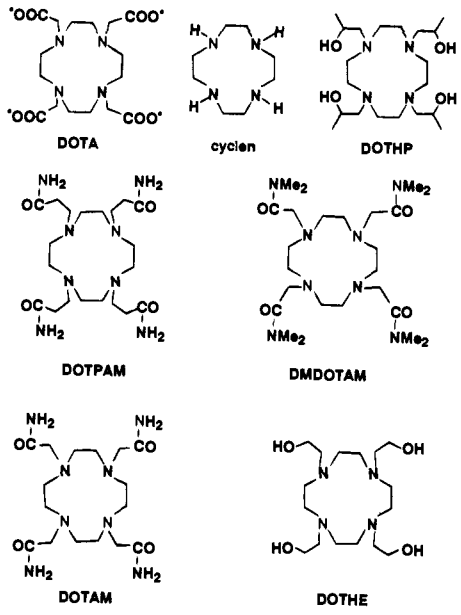

Figure 1. Key to ligands discussed in this work.

the removal of Cd(II). However, selectivity for Pb(II) has been disappointing[4] and has been attributed[4] to the stereochemically active lone pair on Pb(II) leading to a contraction in ionic radius and consequent unfavorable response to the added neutral oxygen donors.

Studies with metal ions in the gas phase show that ligands containing the amide neutral oxygen are stronger donors than alcoholic or ethereal oxygen donors.[8] The small amount of data on formation constants available in the literature[16] also shows that ligands containing acetamide groups are stronger complexing agents than their analogues containing 2-hydroxyalkyl groups. Morrow *et al.*[17] have reported on the complexing properties of a cyclen-based ligand containing *N*-propionamide donor groups (DOTPAM in Figure 1), whose lanthanide complexes may be of potential use in the cutting of RNA at specific sites. This ligand forms six-membered chelate rings on complex formation, so that it is not well suited to complexing large metal ions such as lanthanides. Thus, the DOTPAM complexes of the lanthanides are rapidly hydrolyzed in water.[17] Morrow *et al.*[18,19] have also investigated lanthanide complexes of cyclen-based ligands with 2-hydroxyalkyl pendent groups. Parker *et al.*[20] have briefly reported on the complexing properties of a cyclen-based ligand with *N,N*-dimethylacetamide donor groups on the nitrogen donors (DM-DOTAM). In light of the fact that both Cd(II) and Pb(II) are large[21] metal ions, it seems that *N*-acetamide groups would give a cyclen-based ligand (DOTAM in Figure 1) superior to DOTPAM for the purposes of complexing large metal ions, since acetamide donor groups lead to five-membered chelate rings, while propionamide donor groups lead to six-membered chelate rings. Similarly, the acetamide oxygen donor is a much stronger donor than the alcoholic oxygen, so that DOTAM should be superior to DOTHP for the purposes of complexing the large Cd(II) and Pb(II) ions.

A point of interest with octadentate ligands such as DOTA or DOTAM is what happens as metal ions vary in size. Thus, the Zn(II) ion is possibly too small (ionic radius[21] = 0.74 Å) to coordinate to DOTAM in an octadentate fashion, and the question remains as to what happens to any non-coordinated donor groups. At the other end of the size scale, very large metal ions such as Pb(II) (ionic radius = 1.18 Å) might coordinate extra waters to achieve a coordination number higher than eight. The DOTAM complexes gave good quality crystals of complexes of metal ions ranging in size from the relatively small Zn(II) ion through Cd(II), Ca(II), and Hg(II) and up to the very large Pb(II) ion. As is reported here, the crystal structures of the DOTAM complexes were quite unprecedented, displaying a novel response to the problem of metal ions that are slightly too small for full coordination of all eight donor atoms of a ligand such as DOTAM. The structures obtained suggest a novel mechanism for the helicity interchange in DOTAM complexes that was studied by ^{13}C NMR.

We report here the synthesis of DOTAM, a thermodynamic study of its complexing properties with Ca(II), Sr(II), Ba(II), Zn(II), Cd(II), Hg(II), Pb(II), La(III), Gd(III), and Cu(II), a crystallographic study of its complexes with Zn(II), Ca(II), and Cd(II), a molecular mechanics analysis of the structures of DOTAM complexes, and a ^{13}C NMR study of the rates of helicity interchange of the complexes in solution. A preliminary report on this work has appeared recently.[22]

Ligand design for biomedical applications has become of steadily increasing importance,[6,23,24] with applications ranging from Gd(III) complexes used in MRI[25] to Mn(II) complexes used as superoxide dismutase mimics.[26] This study represents a continuing effort to uncover the factors that control metal ion selectivity, so as to improve the ability of researchers in the field to design ligands for specific complexation of metal ions.

Experimental Section

Materials: Synthesis of DOTAM [1,4,7,10-Tetrakis(acetamido)-1,4,7,10-tetraazacyclododecane]. The ligand cyclen was synthesized according to the method of Richman and Atkins.[27] The ligand DOTAM was synthesized by refluxing a mixture of cyclen (2 g, 0.012 mol), chloracetamide (4.5 g, 0.048 mol), and triethylamine (5 g, 0.049 mol) in ethanol (40 mL) for 4 h. After cooling, the white powder which precipitated was filtered off, washed twice with ethanol (5 mL), and dried at 100 °C under reduced pressure. Yield 28%. NMR (D_2O): 2.59−2.81 ppm (16H, s, N-CH_2-CH_2-N), 3.08−3.27 ppm (8H, s, N-CH_2-CO). Anal. Calcd for $C_{16}H_{32}N_8O_4$: C, 47.99; H, 8.05; N, 27.98. Found: C, 47.55; H, 8.13; N, 27.89.

Synthesis of the Metal Complexes. The general synthetic method involved addition of the metal perchlorates to a molar equivalent of the ligand in methanol/water.

(a) Synthesis of [Cd(DOTAM)]$(ClO_4)_2$·2H_2O (1). The ligand (0.2009 g, 0.502 mmol) in 80% methanol was refluxed, and Cd$(ClO_4)_2$·6H_2O (0.2315 g, 0.552 mmol) in methanol (6 mL) was added dropwise. After an additional 2 h of reflux, the solution was cooled and ethanol (30 mL) was added. A white powder which precipitated when the solution was stirred overnight, was recrystallized from water and dried under vacuum. Anal. Calcd for $C_{16}H_{32}N_8CdCl_2O_{12}$·2$H_2O$: C, 26.05; H, 4.80; N, 15.14. Found: C, 26.06; H, 4.79; N, 14.79.

(b) Synthesis of [Ca(DOTAM)]$(ClO_4)_2$·2H_2O (2). The ligand (0.3235 g, 0.808 mmol) was dissolved in 80% methanol (20 mL) and refluxed. Calcium perchlorate (0.2123 g, 0.888 mmol) in methanol

(16) Martell, A. E.; Smith, R. M. *Critical Stability Constants*; Plenum: New York, 1974, 1975, 1976, 1977, 1983, 1989; Vols. 1−6.
(17) Morrow, J. R.; Amin, S.; Lake, C. H.; Churchill, M. R. *Inorg. Chem.* **1993**, *32*, 4566−4572.
(18) Morrow, J. R.; Chin, K. O. A. *Inorg. Chem.* **1993**, *32*, 3357−3362.
(19) Chin, K. O. A.; Morrow, J. R.; Lake, C. H.; Churchill, M. R. *Inorg. Chem.* **1994**, *33*, 656−664.
(20) Kataky, R.; Matthes, K. E.; Nicholson, P. E.; Parker, D.; Buschmann, H. J. *J. Chem. Soc., Perkin Trans. 2* **1990**, 1425−1432.
(21) Shannon, R. D. *Acta Crystallogr., Sect. A* **1976**, *A32*, 751−767.
(22) Carlton, L.; Hancock, R. D.; Maumela, H.; Wainwright, K. P. *J. Chem. Soc., Chem. Commun.* **1994**, 1007−1008.
(23) Sadler, P. J. *Adv. Inorg. Chem.* **1991**, *36*, 1−48.
(24) Jurisson, S.; Berning, D.; Jia, W.; Ma, D. *Chem. Rev.* **1993**, *93*, 1137−1156.
(25) Lauffer, R. B. *Chem. Rev.* **1987**, *87*, 901−927.
(26) Riley, D.; Weiss, R. H. *J. Am. Chem. Soc.* **1994**, *116*, 387−388.
(27) Richman, J. E.; Atkins, T. J. *J. Am. Chem. Soc.* **1974**, *96*, 2268−2270.

(96 mL) was added dropwise and refluxing continued for 2 h. The solvent was reduced to a third, and ethanol (30 mL) was added and stirring continued for an additional 2 h at room temperature. The complex precipitated out and was filtered off and washed twice with ethanol (20 mL). The product was then recrystallized from water, and the crystals that formed were dried under vacuum. Anal. Calcd for $C_{16}H_{32}N_8CaCl_2O_{12}\cdot 2H_2O$: C, 28.45; H, 5.37; N, 16.59. Found: C, 28.79; H, 5.55; N, 16.75.

(c) **Synthesis of [Zn(DOTAM)](ClO$_4$)$_2$·2H$_2$O (3).** The ligand (0.2097 g, 0.524 mmol) in 80% methanol (25 mL) was refluxed, and a solution of $Zn(ClO_4)_2\cdot 6H_2O$ (0.2145 g, 0.576 mmol) in methanol (6 mL) added dropwise. After being refluxed for an additional 2 h, the solution was cooled, ethanol (30 mL) was added, and the solution was stirred overnight. The precipitate was then recrystallized from water, and the crystals that formed were dried under vacuum. Anal. Calcd for $C_{16}H_{32}N_8ZnCl_2O_{12}\cdot 2H_2O$: C, 27.42; H, 5.18; N, 15.99. Found: C, 27.52; H, 4.83; N, 15.78.

X-ray Crystallography. Colorless plates of **1**, **2**, and **3** were mounted on glass fibers at room temperature. Preliminary examination and data collection were performed for **1** (at room temperature) on a Rigaku AFC5 (oriented graphite monochromator; Mo Kα radiation) diffractometer and for **2** and **3** (both at 193°K) on a Siemens R3m (oriented graphite monochromator, Mo Kα radiation) diffractometer. Cell parameters were calculated from the least-squares fitting for 25 high-angle reflections ($2\theta > 15°$) for all samples. For all crystals ω scans for several intense reflections indicated acceptable crystal quality.

Data were collected for 5.0 to 50.0° 2θ for **1** and **2**, and for 4.2 to 50.0° 2θ for **3**. The scan width for data collection for **2** was 2.0° in ω with a variable scan rate between 2 and 15 deg/min, and the scan width was calculated for **1** by the formulas $1.575 + 0.3 \tan(\theta)$. For **1** the weak reflections were rescanned (maximum of two rescans) and the counts for each scan were accumulated. The three standards, collected every 97 reflections for **2** and **3**, and every 150 reflections for **1**, showed no significant trends. Background measurement for **1**, **2**, and **3** was accomplished by the stationary crystal and stationary counter technique at the beginning and the end of each scan for half the total scan time.

Lorentz and polarization corrections were applied to all collected reflections. A semiempirical absorption correction was applied to all data sets. The structures were solved by Direct Methods[28] for **1**, **2**, and **3**. The structures were refined by employing the programs SHELXTL-PLUS[29] for **2** or SHELXL-93[30] for **1** and **3**. Full-matrix least-squares anisotropic refinement for all non-hydrogen atoms for all structures yielded acceptable residual values at convergence. Hydrogen atoms were placed in idealized positions with isotropic thermal parameters fixed at 0.08 Å^2 except in the case of hydrogens bound to water molecules that were located in the electron density maps. As is commonly the case, the perchlorate ions were found to be disordered for **1**. The disorder was modeled by fitting two partially occupied perchlorate anions in such a way as to share their common chloride atom. The two disordered anions were then restrained to idealized perchlorate interatomic distances. For **2** a perchlorate anion was found to be disordered between two sites with a water occupying one of the sites when the perchlorate was not present. The two sites were modeled with idealized perchlorates at one-half site occupation. The above disordered models were then employed in the structure refinement for **1** and **2**. The large thermal parameters associated with the perchlorates are attributed to the disorder and the difficulty of fitting the idealized anions to the disorder. The perchlorates of **3** did not appear to be seriously disordered.

The absolute configuration of **1** was confirmed by the Flack test.[31] Neutral atom scattering factors and anomalous scattering factors were taken from the International Tables for X-ray Crystallography: Vol. C32 for **1** and **3** Vol. IV for **2**.[33] The atomic coordinates for **1**, **2**, and **3** are given in Tables 2, 4, and 6, and selected bond lengths and angles are given in Tables 3, 5, and 7. Drawings of the complex cations of **1**, **2**, and **3**, showing the numbering scheme, are shown in Figures 2, 3, and 4.

NMR Studies. $^{13}C(^1H)$ NMR spectra were recorded in D_2O or DMF-d_7 solution at 50.32 MHz using a BRUKER AC 200 FT NMR spectrometer locked on deuterium. Chemical shift values are referenced either to internal methanol as 49.00 ppm or to the central peak of the upfield multiplet of DMF-d_7 taken as 29.82 ppm. Sample temperature was controlled by a Bruker B-VT1000 variable-temperature unit to within about 0.5 K.

Molecular Mechanics Calculations. Molecular mechanics (MM) has been successful[34-38] in explaining phenomena in inorganic chemistry, so that MM was applied to the unusual structures of DOTAM complexes. The program SYBYL[39] was used, running on a Silicon Graphics Indigo computer, to model the observed structures using the TAFF force field[40] present in SYBYL with addition of parameters to describe the M−O and M−N bonds. A M−N and M−O force constant[41] of 200 kcal·mol^{-1}·Å^{-1} was used for the M−L bonds, and M−L bond lengths were varied as described in the Discussion section to model what happens to the structure of the DOTAM complex as the metal ion size is varied. The geometry around the metal ion was determined by van der Waals repulsion between the donor atoms and forces within the ligand, as all L−M−L force constants were set to zero. The M−O−C and M−N−C angle bending constants were assigned values of 0.005 kcal·mol^{-1}·deg^{-1}, and the ideal angles were taken to be 109.5°.

Stability Constant Determinations. The protonation constants and stability constants were determined for DOTAM by glass electrode potentiometry at 25 °C in 0.1 M $NaNO_3$, as described previously,[1-7] and are shown in Table 8. Potentials were measured on a RADIOMETER PHM 84 pH meter using G202B glass electrodes which were calibrated in acid−base titrations covering the pH range 2 to 12. The DOTAM complexes of Zn(II), Ca(II), Sr(II), and Ba(II) were labile enough that their formation constants could be studied by conventional glass electrode techniques. The rates of equilibration of the DOTAM complexes of La(III) and Gd(III) were rather slow, and an out-of-cell technique was employed in which solutions corresponding to different points in a conventional acid−base titration were prepared and allowed to equilibrate for a few days in a water bath thermostated to 25 °C. The pH values of these solutions were recorded at intervals until no further drift in pH reading was apparent. For Cu(II), the formation constant of the complex was too high too allow for study by glass electrode potentiometry, since complex formation was complete down to pH values well below 2. It was possible to study the complex formation equilibrium by observing the intensity of the d−d band in the Cu(II) DOTAM complex in the 600-nm region of the spectrum as a function of pH in the pH region 0.3 to 1.0, as described previously[42] for complexes of Cu(II) with tetraaza macrocycles. For Hg(II), the complex was too stable to allow for glass electrode determination of log$K$, and this was carried out using a Hg electrode plus Ag/AgCl reference electrode as described previously.[43] Attempts were made to measure logK_1 for Cd(II) and Pb(II) with DOTAM, first by glass

(28) Sheldrick, G. SHELXS-86 Program for Crystal Structure Solution, Institut fur Anorganische Chemie der Universitat, Tammanstrasse 4, D-3400 Gottingen, Germany.

(29) Sheldrick, G. SHELXTL-PLUS revision 4.11V, SHELXTL-PLUS users manual, Siemens Analytical X-ray Inst. Inc., Madison WI.

(30) Sheldrick, G. SHELXL-93, Program for Crystal Structure Refinement, Institut fur Anorganische Chemie der Universitat, Tammanstrasse 4, D-3400 Gottingen, Germany.

(31) Flack, H. D. *Acta Crystallogr., Sect A* **1983**, *A39*, 876−881.

(32) Hahn, T., Ed. *International Tables for X-ray Crystallography*; D. Reidel Publishing Co.: Dordrecht, Holland, distributed by Kluwer Academic Publishers, 1992; Vol. C, Tables 4.2.6.8 and 6.1.1.4.

(33) Ibers, J. A., Hamilton, w. C., Eds. *International Tables for X-ray Crystallography*; Kynoch Press: Birimingham, England, 1974; Vol. IV pp 99 and 149.

(34) Brubaker, D. W.; Johnson, D. W. *Coord. Chem. Rev.* **1984**, *53*, 1−36.

(35) Hay, B. P. *Coord. Chem. Rev.* **1993**, *126*, 177−236.

(36) Comba, P. *Coord. Chem. Rev.* **1993**, *123*, 1−48.

(37) Hancock, R. D. *Progr. Inorg. Chem.* **1989**, *37*, 187−291.

(38) Hancock, R. D. *Acc. Chem. Res.* **1990**, *23*, 253−257.

(39) SYBYL program, available form TRIPOS Associates, 1699 South Hanley Road, St. Louis, MO 63144.

(40) Clark, M.; Cramer, R. D.; Vanopdenbosch, N. *J. Comput. Chem.* **1989**, *10*, 982−1012.

(41) Hancock, R. D.; Hegetschweiler, K. *J. Chem. Soc., Dalton Trans.* **1993**, 2137−2140.

(42) Thom, V. J.; Hosken, G. D.; Hancock, R. D. *Inorg. Chem.* **1985**, *24*, 3378−3381.

(43) Mulla, F.; Marsicano, F.; Nakani, B. S.; Hancock, R. D. *Inorg. Chem.* **1985**, *24*, 3076−3080.

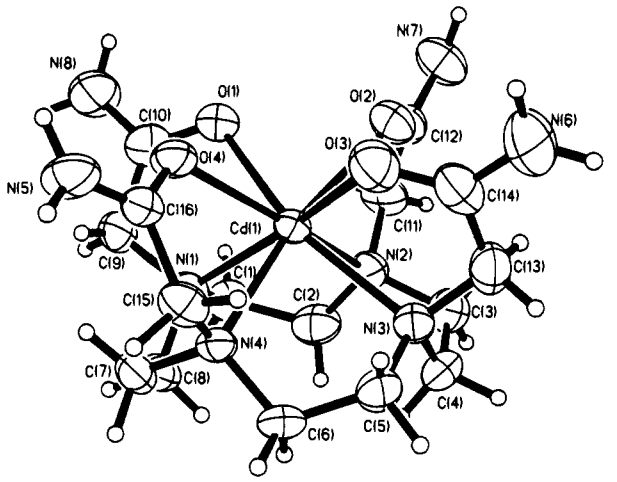

Figure 2. View of the complex cation of $[Cd(DOTAM)]^{2+}$ showing the numbering scheme and thermal ellipsoids drawn at the 50% probability level using the program SHELXTL-PLUS.[52]

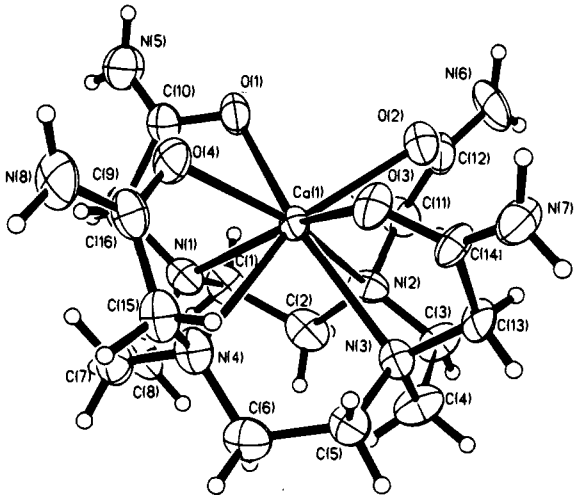

Figure 3. View of the complex cation of $[Ca(DOTAM)]^{2+}$ showing the numbering scheme and thermal ellipsoids drawn at the 50% probability level using the program SHELXTL-PLUS.[52]

electrode potentiometry, then by UV−visible spectroscopy in competition with Cu(II), then by NMR monitoring of the spectrum of the ligand in equilibrium with the metal ion in 0.5 M DCl in D_2O, and finally by polarographic study of the complex in 0.5 M HNO_3. All of these studies showed that the DOTAM complexes of Cd(II) and Pb(II) are not broken down to any measurable extent even in 0.5 M H^+, which means that it is not possible to determine log$K$ for these complexes at this stage, except to place a lower limit on logK_1 of about 19 for Cd(II) and Pb(II) with DOTAM.

Results and Discussion

X-ray Crystallography. The structures of **1**, **2**, and **3** are seen in Figures 2, 3, and 4, respectively. In Figure 5 is shown a view from above the plane of the four oxygen donors of space-filling drawings of the Zn(II), Cd(II), and Ca(II) DOTAM complex cations. The crystal coordinates are seen in Tables 2, 4, and 6, and lists of selected bond lengths and angles are seen in Tables 3, 5, and 7. The striking feature of the structures is the two distinct sets of bond lengths observed for Zn(II) and Cd(II), and possibly also Ca(II). In all of the structures the oxygens of the two short M−O bonds are opposite each other in the approximately square plane defined by the four oxygen donor atoms, as are the two long bonds. For Zn(II) the coordination geometry is best described as six coordinate. The longer two Zn−O distances to the oxygens are 3.33 and 3.13 Å, which are too long to be considered even van der Waals contacts. At the other extreme, the Ca−O bonds show differences in length for the pairs (0.02 Å) that are close to the uncertainties in the Ca−O bond lengths. The Cd(II) structure and also the Hg(II) structure[44] show an intermediate type of structure. The longer Cd−O and Hg−O pairs of bond lengths, averaging 2.64 and 2.78 Å, respectively, are still short enough to be considered bonds, so the point of interest is the nature of these long M−O bonds. Figure 5 suggests that the closeness

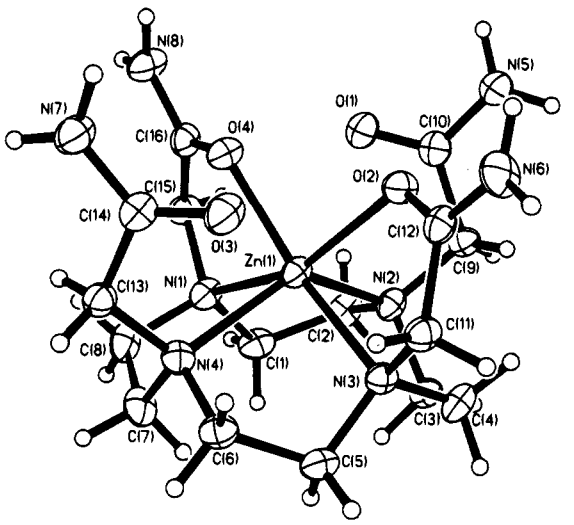

Figure 4. View of the complex cation of $[Zn(DOTAM)]^{2+}$ showing the numbering scheme and thermal ellipsoids drawn at the 50% probability level using the program SHELXTL-PLUS.[52]

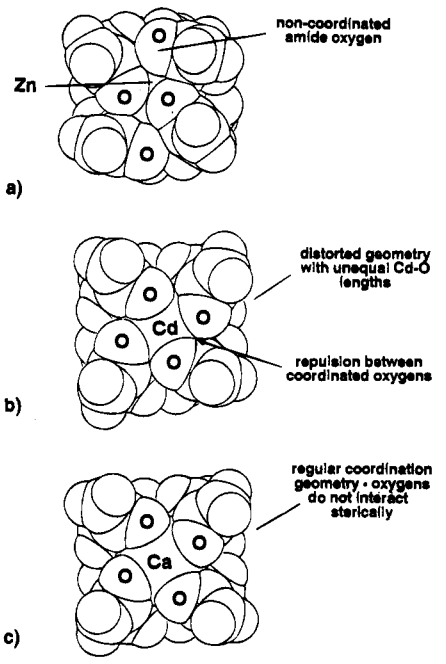

Figure 5. Space filling drawings[52] of (a) the Zn(II), (b) Cd(II), and (c) Ca(II) complexes of DOTAM, viewed from above the coordinated oxygen donors. The drawings show that for the Zn(II) complex the coordination is best described as six-coordinate with the long Zn−O distances averaging 3.23 Å controlled by van der Waals contacts between the amide oxygens. The Cd(II) structure is intermediate between the Zn(II) and more regular Ca(II) structures, with the long Cd(II) bonds averaging 0.30 Å longer than the shorter Cd−O bonds. The short Cd−O bonds may represent normal Cd−O bonds, while the longer bonds may be wholly ionic and controlled by van der Waals contacts with the oxygen donors of the short Cd−O bonds.

(44) Maumela, H.; Hancock, R. D.; Reibenspies, J. To be submitted for publication.

Table 1. Crystal Data for **1**, **2**, and **3**

	1	**2**	**3**
empirical formula	$C_{16}H_{35}N_8O_{13.5}CdCl_2$	$C_{16}H_{36}N_8O_{14.5}Cl_2Ca$	$C_{16}H_{34}N_8O_{13}Cl_2Zn$
formula weight (amu)	738.8	683.5	682.8
crystal color and habit	colorless, plate	colorless, plate	colorless, plate
crystal size (mm)	0.1 × 0.3 × 0.3	0.08 × 0.38 × 0.41	0.11 × 0.33 × 0.41
crystal system and space group	monoclinic, *CC*	monoclinic, $P2_1/c$	triclinic, $P\bar{1}$
cell dimensions			
a (Å)	11.908(2)	14.031(9)	0.490(1)
b (Å)	21.237(3)	11.649(8)	12.464(2)
c (Å)	11.445(2)	17.45(1)	12.998(2)
α (deg)			99.07(1)
β (deg)	102.15(1)	92.10(6)	107.67(1)
γ (deg)			108.42(1)
cell volume (Å^3)	2829.5(8)	2850(8)	1334.1(3)
Z (formula units/cell)	4	4	2
density (calcd) (g/mL)	1.730	1.593	1.700
abs coeff (μ, mm^{-1})	1.037	0.480	1.199
F(000)	1503	1432	708
diffractometer	Rigaku ARC5	Siemens R3m	Siemens R3m
radiation wavelength (Å)	0.71073	0.71073	0.71073
data collection temp (K)	297(2)	193(2)	193(2)
2θ range (deg)	5.0 to 50.0	5.0 to 50.0	4.20 to 50.0
scan type and speed	$\omega/2\theta$, 4 to 16 deg/min	$\omega/2\theta$, 2 to 15 deg/min	$\omega/2\theta$, 2 to 15 deg/min
scan width (deg)	1.575 + 0.3tan(θ)	2.0° + Kα separation	2.0° + Kα separation
background measurements	stationary crystal & counter	stationary crystal & counter	stationary crystal & counter
standard reflcns	3 every 150 reflcns	3 every 97 reflcns	3 every 97 reflcns
index ranges	$0 \le h \le 14$; $0 < k < 25$; $-13 \le l \le 13$	$-16 \le h \le 0$; $-13 \le k \le 0$; $-20 \le l \le 20$	$-11 \le h \le 10$; $-14 \le k \le 14$; $0 \le l \le 15$
no. of reflcns collected	2636	5520	4703
no. of obsd reflcns	2397	2376	3811
observation criterion	$2 \le \sigma(I)$	$4 \le \sigma(I)$	$2 \le \sigma(I)$
abs corr method	semiempirical	semiempirical	semiempirical
T_{max}/T_{min}	0.999/0.920	0.946/0.739	0.912/0.764
structure solution program	SHELXS-86	SHELXS-86	SHELXS-86
structure refinement program	SHELXL-93	SHELXTL-PLUS	SHELXL-93
abs config method	Flack		
abs config parameter	−0.02(4)		
no. of l.s. parameters	435	389	361
$R(F)$ (obsd data)	0.0312	0.0861	0.0590
$wR(F^2)$ (obsd data)	0.0803		
$wR(F)$ (obsd data)		0.0919	
$R(F)$ (all data)	0.0391	0.1509	0.0767
$wR(F^2)$ (all data)	0.0845		0.1756
$wR(F)$ (all data)		0.1094	
$S(F^2)$ (obsd data)	1.0140		0.995
$S(F)$ (obsd data)		3.33	
$S(F^2)$ (all data)	1.0080		0.994
largest and mean l.s. shifts (Δ/σ)	−0.078, 0.006	0.023, 0.001	0.004, 0.001
largest e−density peak and hole (e$^-$/Å^3)	0.871, −0.313	1.370, −0.820	0.912, −1.298

of approach to the metal ion by the oxygen donors of the long M−O bonds in the DOTAM complexes is controlled by van der Waals interactions with the oxygen donors of the short M−O bonds.

Molecular Mechanics Calculations. The MM calculations carried out here were aimed at demonstrating that the closeness of approach of the oxygen donors to the metal ion in the two long M−O bonds observed for the Cd(II) and Zn(II) structures is controlled by van der Waals repulsions with the oxygen atoms coordinated to the metal ion at shorter M−O lengths, as suggested by Figure 5. The forces drawing the oxygens in the long M−O bonds to the metal ion could be purely electrostatic, with a contribution from attractive van der Waals forces. This resembles the way ionic M−O bonds in crown ether complexes of alkali metal ions have been modeled[45] in MM calculations. The oxygen donor atoms are attracted[45] to the alkali metal ions by electrostatic attraction between charges on the metal ion and the donor atoms. The M−O bond lengths are determined[45] by the van der Waals radii of the oxygen donor atom and radius of the metal ion. Because van der Waals repulsive forces dominate the electrostatic attractive forces, the final M−O bond lengths are determined by the radii of the alkali metal ion and the oxygen donor atoms. A MM model was employed in which four nitrogens and two of the oxygens in the DOTAM complexes were represented by a covalent model with ideal bond lengths and M−L force constants of 200 kcal·mol^{-1}. The remaining two oxygen donors were not bonded to the metal ion, and their distance from the metal ion was determined solely by van der Waals interactions between these non-coordinated oxygens and the rest of the complex. It was found that a constant difference between the ideal M−N and M−O bond lengths of 0.10 Å gave a satisfactory account of the structures of the DOTAM complexes. The Zn(II) DOTAM structure was reasonably well reproduced by the above model using ideal Zn−N lengths of 2.17 Å and Zn−O lengths of 2.07 Å. Similarly, this same model with ideal Cd−O and Cd−N bond lengths of 2.35 and 2.45 Å reproduces the structure of [Cd(DOTAM)]$^{2+}$ quite well. A table of MM calculated and observed bond lengths and angles of the bonds involving the metal ions has been deposited as supplementary material.

(45) Wipff, G.; Weiner, P.; Kollman, P. A. *J. Am. Chem. Soc.* **1982**, *104*, 3249−3258.

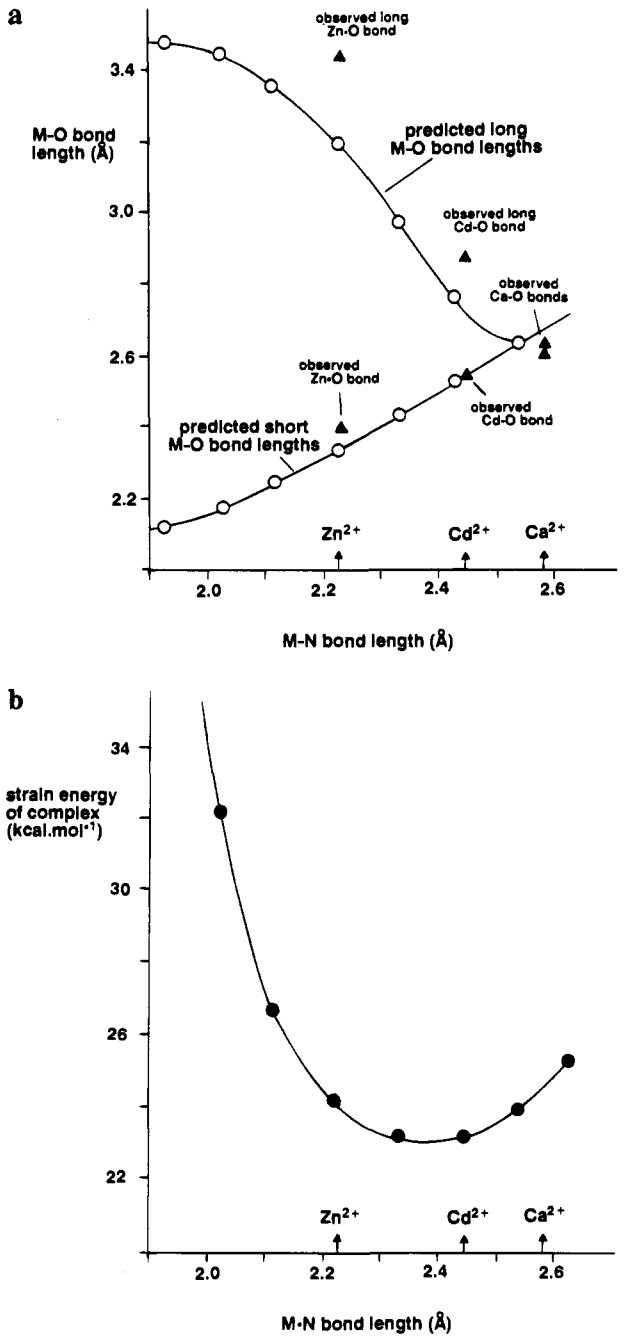

Figure 6. (a) MM calculated long and short M−O bonds (○) in DOTAM complexes, plotted as a function of the MM predicted M−N bond lengths in the complexes as described in the text. The experimental X-ray values for the M−O bond lengths (△) of the Zn(II), Cd(II), and Ca(II) complexes of DOTAM are also plotted on the diagram. X-ray M−O lengths are from this work, and MM calculations were carried out with the SYBYL program.[40] (b) The curve of strain energy for $[M(DOTAM)]^{n+}$ complexes as a function of M−N length, calculated using the MM program SYBYL[40] as described in the text.

Figure 6a shows a plot of the variation of the predicted long and short M−O bond lengths in DOTAM complexes as a function of the energy minimized M−N bond lengths, in the range of M−N bond lengths from 1.9 to 2.6 Å. Superimposed on this diagram are observed short and long M−O bond lengths in DOTAM complexes as a function of observed M−N bond lengths. The observed long M−O bonds in Figure 6a are about 0.1 Å longer than predicted by the MM model used here. This discrepancy could be removed by changes in the TAFF force field used, such as increasing the van der Waals radii of the carbonyl oxygens from 1.52 to 1.7 Å. The significance of this is not clear at present, but it may represent, for example, electrostatic repulsion between the negatively charged oxygen donor atoms which forces them slightly further apart. Figure 6a predicts that the long and short M−O bonds in DOTAM complexes become equivalent with M−N bond lengths of 2.55 Å. The long and short Ca−O bond lengths on Figure 6a are nearly equal, which might be expected from the mean Ca−N bond lengths of 2.59 Å and the prediction by the MM calculations that the four M−O bonds become equal beyond an M−N bond length of 2.53 Å. The MM model suggests that the long M−O bond lengths are largely controlled by repulsive van der Waals interactions with the other donors of the complex. Repulsive van der Waals interactions are the dominant steric interactions in determining structure[13] and override other interactions, so addition of calculated charges to the DOTAM complexes would be unlikely to alter the structure of the complex much. A possibility considered was that the oxygens

Table 2. Atomic Coordinates ($\times 10^4$) and Equivalent Isotropic Displacement Parameters ($Å^2 \times 10^3$) for $[Cd(DOTAM)](ClO_4)_2 \cdot 2H_2O$ (**1**)

	x	*y*	*z*	*U*(eq)[a]
Cd(1)	10006(1)	8936(1)	10006(1)	32(1)
Cl(1)	4428(2)	9331(1)	6178(2)	57(1)
Cl(2)	10588(2)	7311(1)	15753(2)	64(1)
O(1)	11558(6)	8835(3)	12009(6)	51(2)
O(2)	9051(5)	8691(3)	11519(5)	48(1)
O(3)	8254(5)	9725(3)	9808(6)	58(2)
O(4)	10789(5)	9959(2)	10307(4)	43(1)
O(5)	5500(10)	9139(8)	6070(20)	104(8)
O(6)	3660(10)	8826(6)	5900(20)	200(20)
O(7)	4420(20)	9530(10)	7320(10)	150(10)
O(8)	4040(10)	9811(7)	5370(20)	130(10)
O(5′)	4100(30)	9050(10)	7130(20)	190(30)
O(6′)	3500(20)	9480(20)	5300(20)	180(20)
O(7′)	5010(20)	9890(10)	6590(30)	160(20)
O(8′)	5180(20)	8950(10)	5730(30)	170(20)
O(9)	10123(8)	6963(4)	14726(5)	97(3)
O(10)	11570(10)	6980(10)	16330(10)	98(9)
O(11)	9830(10)	7370(10)	16490(10)	100(10)
O(12)	10950(20)	7894(6)	15440(20)	130(10)
O(10′)	11540(20)	7630(10)	15630(20)	240(30)
O(11′)	10770(30)	6930(10)	16740(10)	340(40)
O(12′)	9710(10)	7750(10)	15830(20)	120(10)
O(13)	7780(10)	8960(4)	4195(8)	96(3)
O(14)	5720(20)	10890(10)	7562(20)	91(7)
N(1)	11873(5)	8491(3)	9814(5)	40(1)
N(2)	9843(6)	7795(3)	10185(6)	43(2)
N(3)	8317(6)	8645(3)	8510(6)	41(1)
N(4)	10336(5)	9343(3)	8136(5)	35(1)
N(8)	13374(8)	9070(5)	12707(7)	85(3)
N(7)	9035(7)	8045(4)	13046(7)	63(2)
N(6)	6369(7)	9656(6)	9730(10)	97(3)
N(5)	11063(7)	10854(3)	9393(6)	57(2)
C(1)	11923(7)	7827(3)	10124(8)	47(2)
C(2)	10784(8)	7489(4)	9763(8)	54(2)
C(3)	8703(8)	7600(4)	9487(8)	54(2)
C(4)	8372(7)	7967(4)	8313(7)	54(2)
C(5)	8337(8)	8998(4)	7392(8)	49(2)
C(6)	9525(7)	9047(4)	7154(6)	47(2)
C(7)	11566(6)	9213(4)	8074(7)	42(2)
C(8)	11966(7)	8576(4)	8553(7)	48(2)
C(9)	12768(8)	8847(5)	10603(8)	47(2)
C(10)	12505(8)	8907(4)	11837(8)	48(2)
C(11)	9900(8)	7673(4)	11462(7)	51(2)
C(12)	9277(7)	8181(4)	11999(6)	43(2)
C(13)	7280(10)	8802(5)	8930(10)	52(3)
C(14)	7344(8)	9438(4)	9526(8)	54(2)
C(15)	10166(7)	10015(4)	8175(6)	43(2)
C(16)	10716(6)	10277(3)	9384(6)	36(2)

[a] Equivalent isotropic *U* defined as one-third of the trace of the orthonalized U_{ij} tensor. Estimated standard deviations are given in parentheses.

Table 3. Selected Bond Lengths (Å) and Angles (deg) for [Cd(DOTAM)](ClO$_4$)$_2$·2H$_2$O (**1**)[a]

		Bonds	
Cd(1)−O(2)	2.322(5)	Cd(1)−O(4)	2.362(5)
Cd(1)−N(4)	2.416(6)	Cd(1)−N(3)	2.430(6)
Cd(1)−N(2)	2.441(6)	Cd(1)−N(1)	2.468(6)
Cd(1)−O(1)	2.634(7)	Cd(1)−O(3)	2.649(6)
		Angles	
N(4)−Cd(1)−N(3)	74.4(2)	N(4)−Cd(1)−N(1)	75.0(2)
N(4)−Cd(1)−N(2)	117.4(2)	N(3)−Cd(1)−N(2)	74.9(2)
N(3)−Cd(1)−N(1)	117.9(2)	N(2)−Cd(1)−N(1)	73.5(2)
O(2)−Cd(1)−O(1)	72.3(2)	O(2)−Cd(1)−O(3)	72.8(2)
O(1)−Cd(1)−O(4)	76.4(2)	O(4)−Cd(1)−O(3)	73.1(2)
O(4)−Cd(1)−O(2)	109.7(2)	O(1)−Cd(1)−O(3)	121.4(2)
N(1)−Cd(1)−O(1)	64.3(2)	N(1)−Cd(1)−O(2)	124.9(2)
N(1)−Cd(1)−O(3)	160.5(2)	N(1)−Cd(1)−O(4)	91.7(2)
N(2)−Cd(1)−O(1)	84.2(2)	N(2)−Cd(1)−O(2)	69.9(2)
N(2)−Cd(1)−O(1)	84.2(2)	N(2)−Cd(1)−O(2)	69.9(2)
N(2)−Cd(1)−O(3)	124.1(2)	N(2)−Cd(1)−O(4)	159.4(2)
N(3)−Cd(1)−O(1)	156.6(2)	N(3)−Cd(1)−O(2)	90.4(2)
N(3)−Cd(1)−O(3)	65.2(2)	N(3)−Cd(1)−O(4)	125.4(2)
N(4)−Cd(1)−O(1)	125.8(2)	N(4)−Cd(1)−O(2)	159.6(2)
N(4)−Cd(1)−O(3)	88.3(2)	N(4)−Cd(1)−O(4)	70.6(2)

[a] Estimated standard deviations are given in parentheses.

of long M−O bonds in Cd(II) and Hg(II) complexes occupy the positions that they do for purely steric reasons, and there is no particular attraction to the metal ion. It was found that the amide groups in Cd(II) complexes could be rotated into positions with the oxygens well beyond what could be regarded as bonding distances, actually decreasing the strain energy. This indicates that interaction between the oxygens of the long M−O bonds and the metal ion must provide stabilization to maintain the oxygens in the long M−O bonds close to the metal ion. The most probable factor in stabilizing the long M−O bonds is a weak electrostatic attraction. No attempt was made to model this as the charges calculated on the Cd^{II} and Hg^{II} would at best be highly uncertain. As the long and short M−O bonds become more nearly equal in length, so they become more similar in factors that contribute to their formation and become identical at the coalescence point at a M−N bond length of 2.53 Å. Figure 6b shows strain energy of DOTAM complexes as a function of M−N bond length. This suggests that minimum strain energy will occur with metal ions with M−N lengths of about 2.4 Å, which may account for the high stability of the complexes of Cd(II) with DOTAM reported here.

Thermodynamic Results. Table 8 shows protonation constants and formation constants for DOTAM complexes. As discussed above, only a lower limit for logK_1 for the Cd(II) and Pb(II) complexes could be set. This results partly from the low protonation constants of DOTAM, which make the complexes unusually resistant to demetalation by acid. The low protonation constants arise partly from the electron withdrawing nature of the amide substituents. There may also be a contribution from formation of a complex with the Na^+ ion of the 0.1 M $NaNO_3$ used to maintain ionic strength. The present authors have used $NaNO_3$ as a standard background electrolyte for all their past studies on ligand systems, and so, for purposes of comparison, this was done here also. This is relevant for biomedical studies, since the concentration of Na^+ in plasma is high. However, studies underway in 0.1 M [N(CH$_2$CH$_3$)$_4$]Cl suggest that logK_1 for Na^+ with DOTAM is about 3, which would depress the first protonation constant by about 2 log units in 0.1 M $NaNO_3$. Table 9 shows formation constants of metal ions with ligands based on cyclen, with pendent donor groups. Table 9 shows that DOTAM has the best selectivity for Cd(II) and Pb(II) over Zn(II) of cyclen-based ligands. The selectivity (difference in logK_1 values) of almost 9 log units should make

Table 4. Atomic Coordinates (×10^4) and Equivalent Isotropic Displacement Parameters (Å^2 × 10^3) for [Ca(DOTAM)](ClO$_4$)$_2$·2H$_2$O (**2**)

	x	y	z	U(eq)[a,b]
Ca(1)	6990(2)	4019(2)	1624(1)	24(1)
Cl(1)	8423(3)	−1634(3)	3405(3)	66(2)
Cl(2)	9496(4)	5880(5)	5264(3)	32(2)
Cl(2′)	5000	5000	5000	123(3)
O(1)	6607(5)	4360(6)	2931(4)	37(3)
O(2)	5752(5)	2620(6)	1842(4)	35(3)
O(3)	6009(5)	4367(6)	496(4)	34(3)
O(4)	6765(5)	6071(6)	1648(5)	40(3)
O(5)	8520(8)	−464(8)	3561(6)	85(5)
O(6)	7599(7)	−2094(9)	3704(7)	96(5)
O(7)	9190(8)	−2192(9)	3846(11)	165(8)
O(8)	8584(10)	−1908(12)	2689(8)	145(7)
O(9)	8530(5)	6084(7)	5105(5)	53(3)
O(9′)	4943(24)	5004(82)	5803(5)	500
O(10)	9883(11)	5398(14)	4618(9)	43(6)
O(10′)	5144(44)	6127(24)	4722(55)	500
O(11)	9904(10)	6998(12)	5387(10)	54(7)
O(11′)	5773(19)	4298(17)	4787(26)	500
O(12)	9717(11)	5158(14)	5921(10)	53(7)
O(12′)	4140(11)	4559(72)	4661(33)	500
O(13)	5845(7)	5960(10)	8326(10)	182(9)
O(14)	4872(7)	3516(8)	3577(6)	88(4)
N(1)	8457(6)	4300(7)	2533(5)	34(3)
N(2)	7635(6)	1974(7)	2004(5)	33(3)
N(3)	7488(6)	2908(7)	416(5)	28(3)
N(4)	8340(6)	5123(7)	966(5)	35(3)
N(5)	6981(7)	5308(9)	4010(6)	58(4)
N(6)	5280(6)	1089(8)	2501(6)	55(4)
N(7)	5224(6)	3588(8)	−503(5)	44(4)
N(8)	7073(7)	7778(8)	1144(6)	50(4)
C(1)	8650(8)	3097(9)	2945(6)	37(4)
C(2)	8588(8)	2091(9)	2374(7)	43(5)
C(3)	7667(8)	1250(9)	1309(6)	36(4)
C(4)	8071(8)	1880(9)	639(7)	43(5)
C(5)	8027(7)	3672(9)	−87(6)	34(4)
C(6)	8772(8)	4389(9)	373(7)	42(4)
C(7)	9072(8)	5511(10)	1528(6)	38(4)
C(8)	9311(7)	4567(9)	2112(7)	40(4)
C(9)	8187(8)	5078(10)	3095(6)	39(4)
C(10)	7178(8)	4898(9)	3350(7)	33(4)
C(11)	6940(7)	1492(9)	2512(7)	41(4)
C(12)	5938(8)	1773(10)	2241(7)	39(4)
C(13)	6598(7)	2577(8)	38(7)	34(4)
C(14)	5896(8)	3588(9)	2(6)	30(4)
C(15)	7863(8)	6139(9)	640(6)	37(4)
C(16)	7211(8)	6660(10)	1190(7)	36(4)

[a] Equivalent isotropic U defined as one-third of the trace of the orthogonalized U_{ij} tensor. [b] Estimated standard deviations are given in parentheses.

DOTAM or similar ligands with amide donors ideal for removal of these toxic heavy metal ions in cases of intoxication. Computer modeling of metal ions in blood plasma suggests[4] that a selectivity for Cd(II) or Pb(II) over Zn(II) of four log units would be adequate for drugs for removing Cd(II) or Pb(II) in cases of metal intoxication. It might occur to the reader that mercapto donor groups might provide good selectivity for Cd(II) or Pb(II) over Zn(II), in light of the promising ligands for Cd(II) developed by Jones and co-workers[46] based on sulfur donor ligands. It is not likely that ligands based on mercapto type donor groups will achieve great selectivity for Cd(II) or Pb(II) over Zn(II). The affinities of these three metal ions for mercapto groups are similar, as illustrated by logK_1 values[16] for mercaptoethanol (Cd(II) logK_1 = 6.1; Pb(II), logK_1 = 6.6; Zn(II), logK_1 = 5.7). The MM calculations suggest (Figure 6b) that metal ions with M−N bond lengths of 2.4 Å will coordinate to DOTAM with least steric strain. This corresponds

(46) Casas, J. S.; Sanchez, A.; Bravo, J.; Garcia-Fontan, S.; Castellano, E. E.; Jones, M. M. *Inorg. Chim. Acta* **1989**, *158*, 119−126.

Table 5. Selected Bond Lengths (Å) and Angles (deg) for $[Ca(DOTAM)](ClO_4)_2 \cdot (H_2O)_2$ (**2**)[a]

Bonds			
Ca(1)−O(1)	2.396(8)	Ca(1)−O(2)	2.423(7)
Ca(1)−O(3)	2.395(7)	Ca(1)−O(4)	2.412(7)
Ca(1)−N(1)	2.560(9)	Ca(1)−N(2)	2.625(9)
Ca(1)−N(3)	3.590(9)	Ca(1)−N(4)	2.592(9)
Angles			
N(1)−Ca(1)−N(2)	69.9(3)	N(1)−Ca(1)−N(3)	108.1(3)
N(1)−Ca(1)−N(4)	69.5(3)	N(2)−Ca(1)−N(3)	69.6(3)
N(2)−Ca(1)−N(4)	108.2(3)	O(1)−Ca(1)−O(3)	127.8(3)
O(2)−Ca(1)−O(4)	124.7(3)	O(3)−Ca(1)−O(4)	77.0(2)
N(1)−Ca(1)−O(1)	66.4(3)	N(1)−Ca(1)−O(2)	121.5(3)
N(1)−Ca(1)−O(3)	156.9(3)	N(1)−Ca(1)−O(4)	90.6(3)
N(2)−Ca(1)−O(1)	89.8(3)	N(2)−Ca(1)−O(2)	65.9(2)
N(2)−Ca(1)−O(3)	89.8(3)	N(3)−Ca(1)−O(1)	159.0(3)
N(3)−Ca(1)−O(2)	90.4(3)	N(3)−Ca(1)−O(3)	65.2(2)
N(3)−Ca(1)−O(4)	123.3(3)	N(4)−Ca(1)−O(1)	122.2(3)
N(4)−Ca(1)−O(2)	160.6(3)	N(4)−Ca(1)−O(4)	67.3(3)

[a] Estimated standard deviations are given in parentheses.

Table 6. Atomic Coordinates ($\times 10^4$) and Equivalent Isotropic Displacement Parameters ($Å^2 \times 10^3$) for $[Zn(DOTAM)](ClO_4)_2 \cdot 2H_2O$ (**3**)

atom	*x*	*y*	*z*	*U*(eq)[a]
Zn(1)	4580(1)	2872(1)	2577(1)	20(1)
Cl(1)	1579(2)	6813(1)	1875(1)	41(1)
Cl(2)	2076(2)	899(1)	7577(1)	30(1)
O(1)	8510(5)	4316(5)	3585(3)	38(1)
O(2)	5439(4)	2557(3)	4197(3)	25(1)
O(3)	2526(5)	3124(3)	3945(3)	32(1)
O(4)	5479(4)	4588(3)	3493(3)	23(1)
O(5)	1670(10)	7916(6)	2400(10)	132(3)
O(6)	1760(10)	6940(10)	859(5)	124(3)
O(7)	92(7)	5913(5)	1642(6)	82(2)
O(8)	2893(7)	6586(6)	2538(6)	86(2)
O(9)	1927(7)	2023(4)	7712(5)	62(2)
O(10)	690(6)	25(5)	6656(4)	56(1)
O(11)	3476(5)	988(4)	7339(4)	49(1)
O(12)	2186(5)	557(4)	8595(3)	40(1)
O(13)	8399(7)	948(5)	5206(5)	68(2)
C(13)	1647(6)	3659(4)	2239(4)	24(1)
C(14)	2292(6)	3900(4)	3509(4)	23(1)
C(15)	6175(7)	5073(4)	1944(4)	26(1)
C(16)	6151(6)	5382(4)	3114(4)	24(1)
N(1)	4980(5)	3898(4)	1288(3)	24(1)
N(2)	6179(5)	2185(4)	1992(3)	23(1)
N(3)	3209(5)	980(3)	2267(3)	21(1)
N(4)	2078(5)	2755(4)	1670(3)	22(1)
N(5)	9342(6)	3354(4)	4827(4)	34(1)
N(6)	4644(6)	1451(4)	5300(4)	34(1)
N(7)	2531(6)	4958(4)	4079(4)	31(1)
N(8)	6855(6)	6485(4)	3702(4)	30(1)
C(1)	5515(6)	3230(5)	540(4)	27(1)
C(2)	6756(7)	2832(5)	1227(4)	27(1)
C(3)	5122(6)	946(4)	1335(4)	23(1)
C(4)	4146(7)	322(4)	1960(5)	28(1)
C(5)	1624(6)	629(4)	1352(4)	27(1)
C(6)	918(6)	1557(4)	1533(4)	25(1)
C(7)	2019(7)	2903(5)	547(4)	29(1)
C(8)	3421(7)	3959(5)	650(4)	28(1)
C(9)	7575(6)	2203(4)	2927(4)	23(1)
C(10)	8510(6)	3394(5)	3817(4)	27(1)
C(11)	3026(6)	802(4)	3325(4)	24(1)
C(12)	4481(6)	1673(4)	4318(4)	24(1)

[a] Equivalent isotropic *U* defined as one-third of the trace of the orthogonalized U_{ij} tensor. Estimated standard deviations are given in parentheses. n

to an ionic radius of about 1.0 Å, and it is found that metal ions with ionic radii in this region (Cd^{2+}, Ca^{2+}, La^{3+}, Gd^{3+}) show strong increases in $\log K_1$ on addition of pendent donor groups to cyclen. This is particularly marked with complexes of DOTA with La^{3+} and Gd^{3+}, which probably relates to their

Table 7. Selected Bond Lengths (Å) and Angles (deg) for $[Zn(DOTAM)](ClO_4)_2 \cdot 2H_2O$ (**3**)[a]

Bonds			
Zn(1)−O(4)	2.037(3)	Zn(1)−O(2)	2.162(3)
Zn(1)−N(3)	2.204(4)	Zn(1)−N(2)	2.220(4)
Zn(1)−N(4)	2.253(4)	Zn(1)−N(1)	2.311(4)
Angles			
O(4)−Zn(1)−O(2)	84.3(1)	O(4)−Zn(1)−N(3)	152.1(1)
O(2)−Zn(1)−N(3)	76.0(1)	O(4)−Zn(1)−N(2)	118.7(2)
O(2)−Zn(1)−N(2)	92.0(1)	N(3)−Zn(1)−N(2)	82.1(2)
O(4)−Zn(1)−N(4)	96.4(2)	O(2)−Zn(1)−N(4)	125.6(1)
N(3)−Zn(1)−N(4)	79.8(2)	N(2)−Zn(1)−N(4)	131.8(2)
O(4)−Zn(1)−N(1)	76.7(1)	O(2)−Zn(1)−N(1)	150.7(2)
N(3)−Zn(1)−N(1)	128.6(2)	N(2)−Zn(1)−N(1)	78.4(2)
N(4)−Zn(1)−N(1)	79.0(2)		

[a] Estimated standard deviations are given in parentheses.

Table 8. Formation Constants and Protonation Constants for Complexes of DOTAM[a]

Lewis acid	equilibrium[b]	method[c]	log*K*
H^+	$H^+ + L = HL^+$	pot	7.70(1)
H^+	$H^+ + HL^+ = H_2L^{2+}$	pot	6.21(1)
Cu^{2+}	$Cu^{2+} + L = CuL^{2+}$	UV−vis	16.3(1)
Zn^{2+}	$Zn^{2+} + L = ZnL^{2+}$	pot	10.47(3)
	$ZnL^{2+} + OH^- = ZnLOH^+$	pot	1.08(4)
Ca^{2+}	$Ca^{2+} + L = CaL^{2+}$	pot	7.54(1)
Sr^{2+}	$Sr^{2+} + L = SrL^{2+}$	pot	6.67(2)
Ba^{2+}	$Ba^{2+} + L = BaL^{2+}$	pot	5.35(1)
Hg^{2+}	$Hg^{2+} + L = HgL^{2+}$	pot	15.53(1)
La^{3+}	$La^{3+} + L = LaL^{3+}$	pot	10.35(3)
	$LaL^{3+} + OH^- = LaLOH^{2+}$	pot	6.06(3)
Gd^{3+}	$Gd^{3+} + L = GdL^{3+}$	pot	10.05(3)
Cd^{2+}	$Cd^{2+} + L = CdL^{2+}$	pot	>19
Pb^{2+}	$Pb^{2+} + L = PbL^{2+}$	pot	>19

[a] This work, at 25 °C, 0.1 M $NaNO_3$. [b] Abbreviation, L = DOTAM. [c] Pot = potentiometric.

Table 9. A Comparison of the Formation Constants of Metal Ions with Ligands Based on Cyclen, with Pendent Donor Groups of Several Types[a]

		logK_1 for several pendent donor groups on cyclen			
metal	ionic radius	−H (cyclen)	−CH_2CH· CH_3OH (THP-cyclen)	−CH_2COO^- (DOTA)	−CH_2CO· NH_2 (DOTAM)
Cu(II)	0.57	23.3	19.5	22.2	16.3
Zn(II)	0.74	16.2	13.5	21.1	10.5
Gd(III)	0.94	(8)[b]		24.0	10.1
Cd(III)	0.95	14.3	17.5	21.3	>19
Ca(II)	1.00	3.1	5.7	16.4	7.5
La(III)	1.03	(7)[b]		21.7	10.4
Sr(II)	1.17		5.0	14.4	6.7
Pb(II)	1.18	15.9	15.1	22.7	>19
Ba(II)	1.35		3.7	11.8	5.4

[a] Ionic radii in Å from ref 21, formation constants from refs 4, 16, and 49−51. [b] Estimated from correlation between logK_1 for cyclen complexes and logK_1(NH_3) values.[6]

being the right size for a N_4O_4 donor ligand, as well as their greater affinity for acetate groups. For the neutral oxygen donor the predominant factor is size,[8] so that the increases in logK_1 for the DOTAM complexes relative to the cyclen complexes are similar for all the metal ions of ionic radius close to 1.0 Å. DOTAM does not coordinate Gd(III) particularly strongly and is unlikely to be useful in biomedical applications involving Gd(III). It is unusual that Gd(III) DOTAM is less stable than the La(III) complex. This reflects the smaller size of Gd(III), with the neutral oxygen donors of the amides coordinating better[8] with the larger La(III) ion.

Structural Studies in Solution. To assess the nature of the inner coordination sphere in solution, variable-temperature ^{13}C-

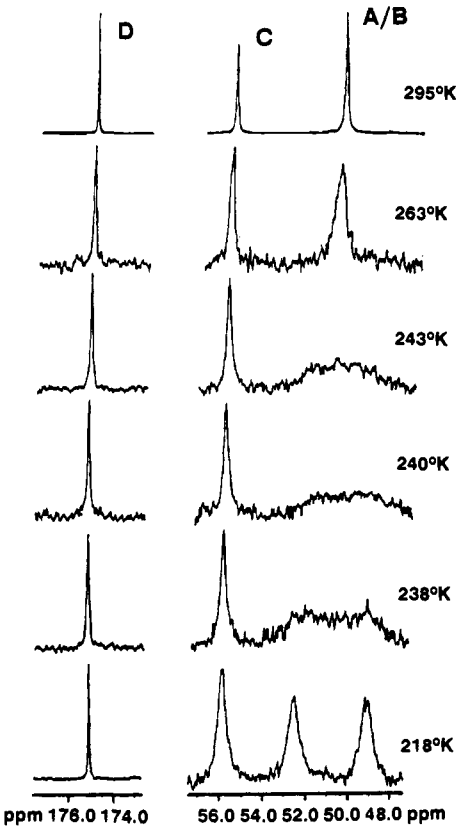

Figure 7. A selection of $^{13}C\{^1H\}$ 50.32 MHz NMR spectra of $[Zn(L)](ClO_4)_2$ in DMF-d_7 at different temperatures.

$\{^1H\}$ NMR studies were conducted on the DOTAM complexes of Zn(II), Cd(II), Hg(II), Ca(II), and Pb(II). These were carried out in D_2O, and for the Zn(II) complex, also in DMF-d_7, for solubility reasons, and to access lower temperatures. The stack of spectra for $[Zn(DOTAM)]^{2+}$, shown in Figure 7, is typical of those shown by all of the complexes of DOTAM in that they indicate equivalence of the four pendant donor groups at all temperatures investigated but inequivalence of the macrocyclic ring carbons, which are differentiated into two groups of four at lower temperatures. The NMR equivalence of the four pendant amide donors on each complex is perhaps surprising in view of the solid state structures presented above, which indicate varying degrees of inequivalence, and must indicate that interchange between the different environments, in which each arm can be seen to exist at different M−O lengths, is too rapid for the individual environments to be distinguished by ^{13}C NMR at 50.32 MHz and temperatures above 218 K. Inequivalence of the ring carbon atoms in molecules of this type has been associated with structures being eight-coordinate and square antiprismatic and is attributed to continual interchange of the helicity of the pendant arm arrangement, as shown in Figure 8, which brings carbon atoms A and B into equivalence on a time-averaged basis.[10,17,18,22] That the Zn(II) complex shows this type of NMR behavior, in spite of its six-coordinate character in the solid state, suggests that even for Zn(II) the regular eight-coordinate structure is not too much higher in energy than the distorted structure seen in the solid state. Thus, it seems likely that the rapid interconversion from having one pair of M−O bonds long and the other pair short to the opposite arrangement would proceed through a more regular structure with all M−O bonds equivalent. The speed of this interconversion indicated by NMR results here would reflect the small difference in energy between the distorted and more regular coordination geometry. It may, in fact, even be that in solution the more regular structure would be dominant. The Na^+ complex with tetrakis(2-hydroxyethyl)cyclen is seven-coordinate in the solid state, but all the oxygen donors are equivalent on the NMR time scale[47] in solution. Rate constants and free energies of activation have been determined at the coalescence temperature for resonances A and B of each complex and are given in Table 10. If approximate correction is made for the different temperatures at which the rate constants have been measured, in accordance with normal Arrhenius type behavior,[48] then it is seen that the rate of helicity interchange follows the order Zn(II) ≫ Hg(II) > Cd(II) > Ca(II) > Pb(II). This ordering correlates well with respect to the difference in length between the longer and shorter pair of M−O bonds, as seen in Table 11, which suggests that such elongation is a necessary prerequisite for the helicity interchange process.

Although elongation of the metal−pendent donor bonds seems necessary for helicity interchange, none the less, the

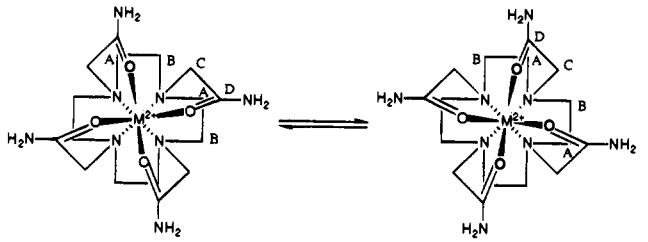

Figure 8. Helicity reversal in the approximately square anti-prismatic complexes of L, which, when occurring rapidly, can lead to equivalence of carbon atoms A and B in the ^{13}C NMR spectra.

Table 10. Rate Constants and Free Energies of Activation for Helicity Reversal in Complexes of DOTAM[a]

M^{2+}	coalescence temp (K)[b]	k (s^{-1})	$\Delta G^{\ddagger}$ (kcal·mol^{-1})
Zn	240	322	11.2
Hg	287	308	13.5
Cd	295	391	13.7
Ca	308	330	14.5
Pb	305	61	15.3

[a] From ^{13}C NMR. [b] At 50.32 MHz.

Table 11. The Difference in M−O Bond Lengths between the Shorter Pair of M−O Bonds and the Longer Pair for Different Metal Ions in Their DOTAM Complexes and the Free Energy of Activation of Helicity Interchange from NMR Spectra

metal ion	mean M−O length[a]		diff	$\Delta G^{\ddagger}$ for rate of helicity interchange[b]
	shorter	longer		
Zn(II)	2.19	3.23	1.04	11.2
Hg(II)	2.41	2.78	0.37	13.5
Cd(II)	2.34	2.64	0.30	13.7
Ca(II)	2.40	2.42	0.02	14.5
Pb(II)			(0.00)[c]	15.3

[a] In Å. M−O lengths from this work, except for Hg(II) and Pb(II), which are still to be published. [b] This work, kcal·mol^{-1}. [c] Pb(II) structure with DOTAM presently being determined. It shows a novel structure with a possible Pb--H−O hydrogen bond to a water molecule. Although the geometry is considerably distorted, probably due to a stereochemically active lone pair on Pb(II), the mean values of the pairs of Pb−O bond lengths for oxygens opposite each other do not show the type of distortion observed for Cd(II) and Hg(II).

(47) Buoen, S.; Dale, J.; Groth, P.; Krane, J. *J. Chem. Soc., Chem. Commun.* **1982**, 1172−1174.
(48) Frost, A. A.; Pearson, R. G. *Kinetics and Mechanism*, 2nd ed.; John Wiley & Sons: New York, 1961; p 22.
(49) Clarke, E. T.; Martell, A. E. *Inorg. Chim. Acta* **1991**, *190*, 27−36, 37−46.
(50) Chaves, S.; Delgado, R.; Frausto da Silva, J. J. R. *Talanta* **1992**, *39*, 249−254.
(51) Cacheris, W. P.; Nickle, S. K.; Sherry, A. D. *Inorg. Chem.* **1987**, *26*, 958−960.

evidence suggests that mechanistically the process is still non-dissociative and presumably, therefore, operates through a cubic structure. That this is the case is suggested by the fast exchange spectra for two [Cd(II) and Hg(II)] out of the three complexes, where it might be expected to be seen, on the grounds that the metal concerned has at least one naturally occurring isotope with $I = {}^1/_2$ [Cd(II), Hg(II), Pb(II)]. The coupling constants measured are $^2J_{C,Cd} = 9.4$ Hz and $^2J_{C,Hg} = 11.2$ Hz. As there is no obvious reason why a similar coupling is not observed in the Pb(II) spectrum, to ^{207}Pb, which has a similar magnetic moment and natural abundance to ^{199}Hg or to $^{111/113}$Cd, it may be that with Pb(II) the helicity reversal is dissociative. However, it cannot be ruled out that either the intensity or the coupling constant for the ^{207}Pb satellites is too small for detection using our present instrumentation.

Conclusions

DOTAM is a powerful ligand for larger metal ions, and it or its derivatives may prove successful for selectively removing toxic metal ions such as Cd(II) and Pb(II). The DOTAM complexes of Zn(II) and Cd(II) are best described as six-coordinate with secondary coordination of the other two oxygen donors, and these structures raise interesting questions about coordination geometry where metal ions are too small for the number of donor atoms present. NMR studies show that the pendent amide groups are equivalent on the NMR time scale, and there is a correlation between rate of helicity interchange and the degree of distortion of the coordination geometry of the complex. The authors are presently conducting animal experiments with DOTAM to evaluate its potential in cases of Cd and Pb poisoning.

Acknowledgment. The authors thank the University of the Witwatersrand and the Foundation for Research Development for generous financial support for this work.

Supplementary Material Available: Tables of complete listing of bond angles and lengths, anisotropic displacement parameters, H-atom coordinates, and equivalent isotropic displacement parameters for $[Zn(DOTAM)](ClO_4)_2 \cdot 2H_2O$, $[Cd(DOTAM)](ClO4)_2 \cdot 2H_2O$, and $[Ca(DOTAM)](ClO_4)_2 \cdot 2H_2O$, plus MM calculated and observed bond angles and lengths for Zn(II), Cd(II), and Ca(II) DOTAM complex (8 pages); list of calculated and observed structure factors (48 pages). This material is contained in many libraries on microfiche, immediately follows this article in the microfilm version of the journal, can be ordered from the ACS, and can be downloaded from the Internet; see any current masthead page for ordering information and Internet access instructions.

JA943740E

(52) Sheldrick, G., XP revision 4.11V *Program for Molecular Graphics*; SHELXTL-PLUS users manual, Siemens Analytical X-ray Inst. Inc., Madison WI, 1992.